Time evolution of observed July-September SST-Sahel climate teleconnection with removed quasi-global effect (1900-2008)

Bernard Fontaine, Marco Gaetani, Albin Ullmann, Pascal Roucou

Time evolution of observed July-September SST-Sahel climate teleconnection with removed quasi-global effect (1900-2008)

Bernard Fontaine[1], Marco Gaetani [2], Albin Ullmann [1], Pascal Roucou[1]

[1] Centre de Recherches de Climatologie, CNRS/Université de Bourgogne, 6 Boulevard Gabriel, 21000 Dijon, France

[2] Istituto di Biometeorologia, IBIMET-CNR, Via dei Taurini 19, 00185 Roma, Italy

Abstract

Using SST, precipitation and atmospheric information, this statistical study revisits the questions of the July-September SST-Sahel teleconnection variability after removing impact of quasi-global SSTs over the period 1900-2008. The eastern Mediterranean and the Indian Ocean dominate the relationship, both in terms of intensity and time stability, with significant values in 52% and 47% of years, respectively. More than two thirds of the rainy seasons classified as dry (wet) and 16/18 (12/15) of those classified as very dry (very wet) are concomitant of negative (positive) differences between the Mediterranean and the Indian Ocean. Correlations with the tropical Atlantic, the Nino area and the western Pacific region are generally lower and less robust, although, in some periods, they can be high with the southern tropical Atlantic.

Telecconnection observed with continental precipitation and the 950 hPa moisture flux field confirmed these results. Positive SST differences between the eastern Mediterranean and the Indian Ocean are synchronous of in phase rainfall excess over the whole Sudan-Sahel due to a strengthening of the convergence between the north-easterly moisture transport from the eastern Mediterranean and the monsoon south-westerly moisture transport from the eastern

equatorial Atlantic. This is associated with changes in the atmospheric circulation along the meridional and zonal planes, mainly (i) a subsidence departure from mid-levels above 10°N-18°N associated with air ascents above the Saharan thermal lows; (ii) upward anomalies on the western and eastern Sahel reinforcing the atmospheric ascents in upper levels; (iii) a low-level subsidence anomaly by 30°E-40°E in agreement with the Indian cooling weakening the normal uplifts; (iv) a reinforcement of the Tropical easterly Jet over 0° -20°E.

1. Introduction

The objective of this study is to revisit the question of the summertime SST-Sahel teleconnection variability along the twentieth-century using both several gridded datasets for describing time evolution of the basic fields (SST, precipitation, atmospheric circulation) and selected key-SST indexes and atmospheric descriptors representative of the West African monsoon.

The question is to what extent have quasi-global SST and basin-scale variations contributed to the observed changes in the teleconnection, i.e., to the long-term evolution of correlation patterns defined at an interannual time step. The purpose is therefore different from previous studies which often have documented this relationship without removing the global warming effect. In this work we have chosen to separate thermal evolutions observed in the different Oceanic basins, including the Mediterranean, from the global scale SST (GSST) influence, regardless of its natural or anthropogenic origin. Removing the GSST-related influence has a significant effect on long-term SST evolution in the Oceanic basins and allows us to separate better basin-scale variability from longer-term evolutions and, therefore, to quantify suitably their relative statistical impacts on Sahelian rainfall. In addition, the investigation of the Mediterranean role in the variability of the Sahelian precipitation on a multi-decadal time-scale represents an outstanding effort in filling this gap in the knowledge

of the West African monsoon teleconnections. Using linear correlations, multiple regressions, composite methods and cluster analyses we discuss the results in terms of statistical significance and time stability over various periods ranging between 1900 and 2008. Furthermore, we conclude by a short analysis of the atmospheric circulation in terms of moisture transport, and large scale divergent meridional and zonal circulation, in order to highlight the association with the SST time evolution.

2. Review of the literature

The relationship between sea surface temperature (SST) fields and summer Sahel rainfall has been studied for a long time, emphasizing the potential role of tropical Oceanic basins (Hastenrath and Lamb, 1977; Lamb, 1978; Lough, 1986; Folland et al., 1986; Palmer, 1986; Nicholson and Nyenzi, 1990; Ward et al., 1990; among many others). Overall these authors showed that warmer (colder) waters southward to the equator -relative to that northward- were often associated with Sahelian drier (wetter) conditions over the Sahel. In particular Folland et al. (1986) have been the first authors who linked Sahelian rainfall long-term variability to the differential SST warming between the hemispheres through the latitudinal location of the ITCZ over the Atlantic. This statistical teleconnection, observed both at the inter-annual and decadal scales, is in good agreement with model results and hence can be interpreted in terms of Oceanic forcing on the tropical circulation. In the Atlantic, for example Hastenrath and Polzin (2010) show that warmer (cooler) surface waters over the tropical North Atlantic accompanied by lower (higher) surface pressure enhance (decrease) the cross-equatorial winds from the Southern Hemisphere and hence precipitation in the Sahel. In the ARPEGE AGCM, the simulated drought is associated with a southward shift of the continental rainbelt over central and eastern Sahel, linked to an inter-hemispheric SST mode, the southern hemisphere Oceans warming faster than the northern ones after 1970 (Caminade and Terray, 2010). Other model experiments (Losada et al., 2009) indicate that

warmer SST anomalies in the equatorial Atlantic lead to a decrease of the local surface temperature gradient, weakening the West African monsoon flow and the surface convergence over the Sahel. Ward (1998) and Joly and Voldoire (2010) state that the main Oceanic sources of seasonal rainfall predictability over West Africa are SST anomalies in the equatorial Pacific, the equatorial Atlantic and the Mediterranean.

Possible causes and impacts of SST variability at longer-term have been also pointed out. Thus Delworth et al. (1993) described thermal impacts of the North Atlantic thermohaline overturning circulation at multi-decadal scales: the resulting SST pattern is known as the Atlantic Multi-decadal Oscillation (AMO; Goldenberg, 2001; Zhang and Delworth, 2006). Bader and Latif (2003) identified the warming of the Indian Ocean -partly due to anthropogenic greenhouse gases (Stott et al., 2000)- as a potential source of Sahelian drying. They suggested that warming trends in the Indian Ocean played a crucial role for the drying trend over the West Sahel from the 1950s to 1990s, while the tropical Pacific's influence is predominantly over the East Sahel and the tropical Atlantic impacts rainfall only along the Guinea Coast. More recently, focusing on the very dry year 1983, Bader and Latif (2009), showed that the Indian Ocean significantly affects inter-annual rainfall variability over the west Sahel. In particular, they provide evidence that the remanence from the strong 1982/1983 El Niño event in this Ocean was the main forcing for the drought observed in 1983 over the Sahel.

Studying the ENSO-Sahel relationship, Janicot et al. (2001) proposed that the existence of periods of weak or strong linkage could result from an interaction with the global decadal scale SST variability, which is able to enhance the impact of the warm ENSO phases after 1980, through an increase in the fill-in of the monsoon trough and a moisture advection deficit over West Africa. In addition, Giannini et al. (2003) related the warming of the low-latitudes waters around Africa to the recent negative precipitation trend in the Sahel,

hypothesizing that the favoured deep convection over the Ocean could weaken the monsoonal convergence over the continent. More generally the drying trend observed in the Sahel from the 1950s to the mid 1980s coincides with marked decadal shifts like those in the Atlantic Multidecadal Oscillation, the Pacific Decadal Oscillation, the low frequency component of the Atlantic Niño and the global temperature (Rodriguez de Fonseca et al., 2010).

The linkage between the local forcing and the remote SST signals implied in the Sahel/SST teleconnection has been also discussed. For example, Rowell et al. (1995) showed that SSTA linked to the Nino/Nina variability impacts indirectly on JAS Sahelian rainfall via atmospheric teleconnection generating SST anomalies in the Atlantic. Rodriguez-Fonseca et al. (2009) presented observational evidence of a change in the Atlantic-Pacific Niños connection since the late 60's. The role of the eastern Mediterranean basin in the determination of the inter-annual variability of the monsoonal precipitation has been highlighted by Rowell (2003) and Fontaine et al. (2009): warm SST anomalies positively affect the Sahelian precipitation in JAS in reinforcing the moisture transport from the Mediterranean across the Sahara and hence the moisture flux convergence over the Sahel.

Thus the SST forcing can be considered as the dominant driver of West African rainfall variability. Conversely it is not the unique factor impacting rainfall in this monsoon region for at least three reasons: (1) atmospheric internal variability contributes strongly to driving the simulated precipitation variability over the Sahel at decadal to multi-decadal time scales (Caminade and Terray, 2010); (2) land surface vegetation processes and dust feedbacks may amplify rainfall anomalies (Biasutti et al., 2008); global warming impacts both multi-decadal SST variability and monsoon circulation (Paethe and Hense, 2004).

Indeed West Africa is sensitive to water vapour and lapse rate, vegetation, surface albedo, clouds and also aerosols. For example, aerosol feedbacks may act to amplify the Ocean-forced component of monsoon circulation: the direct and the indirect effects of

aerosols affect the SST gradients and favour drying at the northern edge of the ITCZ (Biasutti and Giannini, 2006). By contrast, for Kim et al. (2010) aerosol radiative forcing and induced circulation and precipitation cool the Sahel and the southern part of Sahara desert more than the adjacent areas to the north and south. It tends to shift the peak of the meridional temperature gradient northward and consequently the African easterly jet.

In their detailed review of biophysical processes studies for the Sahel area, Xue et al. (2004) present the main land/atmosphere feedbacks and mechanisms exerting a significant impact on the Sahel climate (see for more details Fig. A42 and comments p. 74). In particular, as Zeng et al. show in 1999, they exhibit that interactive vegetation processes must be included in models for simulating correctly the decadal precipitation variability over the Sahel. Moreover, as Charney et al. and Walker and Rowntree show in 1977, Xue et al. (2004) highlight that increases/decreases in albedo lead to the reduction/augmentation in precipitation while less initial soil moisture leads to less precipitation.

About global warming, Paethe and Hense (2004), among other authors, have implied greenhouse-gas driven signals, showing that the partial amelioration of the Sahel drought in recent years may be a sign of a long-term increase in rainfall. For Polyakof et al. (2010) also the current North Atlantic warming is linked to both this multi-decadal variability and long-term climate change (including anthropogenic and natural).

3. Data and Methods

3.1 SST data

The SST data are a 60°N-40°S selection of the extended reconstructed sea surface temperature (ERSST) from the most recently available Comprehensive Ocean-Atmosphere Data Set (COADS) SST data with improved statistical methods allowing stable reconstruction

using sparse data. We will use the ERSST.v3b version which is an improved extended reconstruction over version 2 with no satellite data (more details available in Smith et al., (2007) and at http://www.ncdc.noaa.gov/oa/climate/research/sst/ersstv3.php). Computations of the derived SST signals of global and regional scale will be presented in section 3.1.

3.2 Rainfall data

The Sahel rainfall index used in this study is the precipitation anomaly defined by the NOAA NCDC Global Historical Climatology Network. This index refers to the 1950-79 climatology and is averaged over a 20°-10°N, 20°W-10°E West-African window (see jisao.washington.edu/data/sahel for more details). The correlation coefficients between the July-September values of this rainfall index and other Sahel indices used in the literature, such as those defined by Lamb (1978), Bell and Lamb (2006) and Nicholson (1979) are positive and significant at p=0.01 regarding to a Monte Carlo procedure taking into account autocorrelation in the series : r=0.89 with the Nicholson's Sahel index over the common period 1901-1994 and r= 0.58 with the Lamb's time series over the common period 1941-2009.

In addition two data sets have been selected for enlarging the window:

(1) The high-resolution CRU TS 2.1 data-set to focus more on different West African sub-regions: these data comprise 1224 grids of observed climate, for the period 1901-2002, and cover the global land surface at 0.5 degree resolution (see New et al, 2002 and Mitchell et al, 2004).

(2) The last available version of the VASClimO 50-Year dataset (1951-2000) from the Global Precipitation Climatology Centre (GPCC) because only this version supplies gridded time-series of monthly precipitation at 1 degree resolution for climate variability and trend studies

(Beck, Grieser and Rudolf, 2005): it is based on data selected with respect to a (mostly) complete temporal data coverage and homogeneity of the time-series (http://gpcc.dwd.de).

3.3 Atmospheric data

Two regional atmospheric signals representative of the African monsoon circulation in July-September have been defined between 20°W and 30°E through the NCEP/NCAR reanalyses over the period 1950-2008: (i) the vertical velocity at 400 hPa (Pa/s) over 15°N-10°N (ω, the vertical velocity in Pa/s) which is directly linked to moist convection processes at Sahelian latitudes; (ii) the West African Monsoon Index (WAMI; Fontaine et al., 1992) between 15°N and 5°N which is a proxy of the monsoon cell intensity at regional scale: WAMI is the difference between the standardized values of the wind modulus at 925 hPa and of the zonal wind at 200 hPa averaged in the considered domain.

In addition, the atmospheric moisture flux at 950 hPA and the divergent (irrotational) part of the horizontal wind at the different pressure levels of the troposphere have been computed through the monthly NOAA-CIRES 20th Century Reanalysis. This dataset is based on surface pressure observations assimilated every six hours in an atmospheric model, and time-evolving sea surface temperature and sea ice concentration fields as boundary conditions. The model used the state-of-the-art atmospheric general circulation model, a 2008 updated experimental version of the atmospheric component of NCEP's operational Climate Forecast System model (Saha et al., 2006). It has a spatial resolution of nearly 200-km in the horizontal (corresponding to a truncation T62) and 28 vertical levels. The data are provided at a 2°*2° latitude-longitude resolution (more details in Compo et al. (2006) and at http://www.esrl.noaa.gov/psd/data/gridded/data.20thC_ReanV2.html). The dataset will be used over the period 1920-2008 to limit time variations of the information anisotropy at the very beginning of the century and during the first world war.

3.4 Statistical methods

Statistical links are presented through linear correlations, multiple regressions, composite methods and cluster analyses. The correlation significance is estimated through permutation tests which do not require specific distributions such as normality and give more accurate P-values than usual statistical tests. Correlation and P-values at 0.05 and 0.01 will be indicated in text and tables by one or two '*', respectively. Multiple regressions have been conducted with cross validation techniques. Composite results are tested using paired Student-t-test. Cluster analyses use a k-means algorithm minimizing the sum, over all clusters, of the within-cluster sums of point-to-cluster-centroid distances: each procedure has been repeated 100 times, each time with a new set of initial centroids.

4. Correlation patterns

Let us recall first the basic SST/Sahel correlation patterns observed over different periods at quasi-global scale: 1900-1949, 1950-1970, 1971-1990 and 1991-2008 (figure 1). During the first half of the 20th century (Figure1a), a few Oceanic regions exhibit a statistical link with the Sahelian rainy seasons, i.e., the equatorial, southern and NW zones in the Pacific, some areas in the extratropical Atlantic in the Indian Ocean, along with the whole Eastern Mediterranean and Black Sea. Interestingly, no signal is encountered in the tropical Atlantic.

After 1950 (Figure 1b-d), the coefficients increase and involve larger Oceanic regions in the Tropics, such as the eastern and central parts of equatorial Pacific, the Indian Ocean and the eastern Atlantic (negative correlations), the Western equatorial Pacific, the Western equatorial Atlantic and the Mediterranean (positive correlations). In the extratropical region, positive coefficients are also registered by 40°N in the Pacific and Atlantic.

In fact, figure 1 illustrates well the time instability of correlation patterns and reveals that changes at basin scale are obvious everywhere. Thus, the negative correlations observed in the 50s and 60s (figure 1b) in the equatorial Atlantic and Indian Ocean, disappear in the 70s and 80s (figure 1c) and become positive on the most recent period (figure 1d). It is thus interesting to separate this quasi-global evolution from proper SST variability in the different basins. There are several ways for doing that.

In this study, a quasi Global SST (GSST) index, weighted by the square root of cosine of latitudes and averaged between 60°N and 40°S is first defined as an Oceanic proxy of the global SST evolution. $GSST_{(time)} = \Sigma (SST_{(lat, lon, time)} . \cos(lat)^{0.5}) / n$, where n is the number of grid-points considered. The GSST influence is then removed to each line to better capture regional signals that can be considered as independent from global evolution: $SST'_{(lat,lon, time)} = SST_{(lat, lon, time)} - GSST_{(time)}$. Such a procedure is more natural and appropriate than removing a simple linear trend not observed over the reference period. Although GSST is defined at a monthly scale, its long-term evolution (see the caption and figure 2a) is similar to the GW signal based on yearly averaged global SSTs, between 60°N and 45°S because of lower SST data coverage, shown by Mohino et al. in 2010.

5. Time evolution of key-SST regional indices versus Sahel rainfall

Nine regional SST indexes representative of the regions linked to Sahel rainfall variability (figure 1) are now defined as a snapshot of SST evolution since 1900, by averaging the values over:

- the Western Mediterranean (WMED: 32°N-44°N; 6°W-15°E) and Eastern Mediterranean (EMED: 32°N-44°N; 15°E-36°E) basins, and the whole Mediterranean (MED)
- the Northern Tropical Atlantic (TNA: 5°N-24°N; 50°W-15°W), the Southern Tropical Atlantic (TSA: 20°S-0°; 30°W-10°E) and the TNA-TSA differences. The correlation between

TSA and an equatorial Atlantic index computed over (3°N-3°S and 20°W-0°) is positive, high and significant (r=+0.86**).

- the Tropical Indian Ocean (IND: 24°S-24°N; 35°E-90°E), the West Pacific Region (WPR: 20°N-20°S; 100°E-160°E) and the Nino 3.4 region (Nino: 5°S-5°N; 170°W-120°W)

Finally a detrended and unsmoothed version of the Atlantic Multi decadal Oscillation (AMO) is added since Goldenberg et al. (2001), Zhang et al.(2006) and Polyakov et al. (2010), among others, have shown the role of AMO on observed multidecadal variations of SSTs and Sahel rainfall. We use the NOAA PSD AMO, from the Kaplan SST dataset V2 (5x5) refering to the area weighted average over the North Atlantic (0°-70°N).

Figure 2 presents time variability of these SST signals since 1860 with superimposed July-September Sahelian rainfall time series since 1900. The quasi global SST field evolution (GSST in figure 2a) is marked by two major warming phases occurring from 1910 to 1940, then from 1975 to present. Notice that the AMO time series (thin curve) which describes an apparent 60-80 year pseudo-cycle in SSTs displays prolonged periods of warming and cooling often in phase and correlated with GSST (r=+0.57**).

In the Mediterranean, SST evolutions in the Western and Eastern basins (WMED, EMED dashed and solid curves in figure 2b) exhibit marked covariations in the last 50 years with a noticeable cooling from 1960 to 1980 concomitant of the Sahelian dry phase (bars) followed by a clear warming, concomitant of the recent Sahel rainfall recovery. In fact, EMED remains positive (negative) from 1912 to 1970 (1970 to 1997) during the long period of Sahelian rainfall excess (deficit).

In the tropical Atlantic (figure 2c) the northern (dashed curve) and Southern (solid) anomalies exhibit often inverse polarities as in years 1917-25, 50-60, 67-75 which can favour inter-hemispheric SST anomaly gradient able to modify the location of the ITCZ. This inverse

evolution, associated with the dipolar pattern between the northern and southern basins is well captured by the TNA-TSA difference (circles).

SST evolutions in the Indian and Pacific Oceans (IND, Nino and WPR in figure 2d) also show a strong variability all along the period. In particular the IND series (solid curve) displays a succession of years with negative values (1925-1960) followed by a warm phase since 1960, while the Nino (curve with circles) and WPR (dashed curve) series are negatively correlated all along the period (r=-0.72**). This inverse correlation is due to the well known El Nino Southern Oscillation seesaw of reversing surface air pressure between the eastern and western tropical Pacific.

Let us now display in table 1 the significant correlation coefficients registered between these SST indexes and rainfall amounts over different African regions, i.e., the western, central and eastern parts of the Sahelian (10°N-20°N and Guinean (5°N-9.5°N) belts. The results show that (i) the Sahelian belt is more affected by the teleconnection than the subequatorial zone, (ii) connections imply nearly all indexes except AMO and TNA, (iii) small differences are recorded between the western, central and eastern African windows. Overall, correlations are negative, except those implying the Mediterranean basins, and the equatorial/southern tropical Atlantic. This is well confirmed through composite analyses (table 2) retaining only the SST anomalies exceeding |0.5| standard-deviation over a larger period (1900-2008). Noteworthy, the teleconnection is rather linear but stronger with the Mediterranean index (correlated positively in 76% of occurrences), and with IND (70%) and Nino (63%), both correlated negatively with Sahelian rainfall. In the Atlantic TSA exhibits a negative relationship in 57% of occurrences.

6. Time instability of the SST/Sahel teleconnection

To better focus on this aspect, already noticed in figure 1 and section 4, figure 3 displays 20-year running correlations registered with each SST index. Several observations may be made.

1. The GSST and AMO series change continuously and are significant in less than 10% of occurrences: with GSST correlation series (bold curve in Fig. 3a) often negative in the 60s, 70s and 80s, i.e., a period of increasing drought occurrences over Sahel in agreement with Giannini et al. (2003). The lack of correlation with AMO is not surprising regarding the period and Hodson et al. (2010) who show that, in contrast to some studies, the Atlantic Multidecadal Oscillation was not the primary driver of recent reductions in Sahel rainfall. However, significant correlations are observed in the 50s, and are consistent with a northward displacement of the ITCZ and wet anomalies in the Sahel (Mohino et al., 2010).
2. The relationship involving WMED is rather low and rarely significant (13%): it is significant in the 60s and 70s then after 1982 (thin curve, fig 3b). In contrast, except in the 40s and 50s, EMED (bold curve, fig. 2b) shows a quasi-persistent teleconnection in more than 50% of years. The teleconnection is in good agreement with Rowell (2003), Raicich et al. (2003) and Fontaine et al. (2009) who showed observational and model evidence of a thermal forcing of the Mediterranean -with maximum amplitude in the eastern basin- on the African monsoon leading to increasing moisture convergence (and therefore rainfall) over Sudan-Sahel latitudes through changes in the southward moisture advection across the eastern Sahara by the flow.
3. The connection with TNA is rarely significant (4%) and only observed during the wet 50s and 60s (dashed curve in fig 3c). The negative correlation with TSA is more recurrent (20%), primarily in the 40-70s. As a result, the association with the dipolar pattern is positive and significant during the same period (15%, dash-dotted curve with circles). This is in good agreement with Janicot et al. (2001) who showed that during the transition

between the wet sequence to the dry one, the correlations between the Sahel rainfall and the tropical Atlantic dipole were the highest.

4. The statistical relationship with IND and Nino is negative. Figure 3d shows that the correlation is more often significant with IND (47%, chiefly between 1920 and 1975) than with Nino (28%, mainly from 1900 to 1930, and after 1968). Indeed, IND and Nino are not significantly correlated together over the total period (+0.13) or over subperiods before/after the 1976-1977 climate shift in the tropical Indian-Pacific region (+0.12, +0.13, respectively). The correlation with Nino confirms results of Joly and Voldoire (2009) and Rodriguez-Fonseca et al. (2010) and is partly due to the Atlantic Niño- Pacific La Niña relationship starting after the 70's found by Polo et al. (2008) and Rodriguez-Fonseca et al. (2009). It is also noteworthy that the 20-year running mainly deemphasizes the information in past 20 years, which is an important rainfall recovery period. Figure 2, which only eliminates the time variability < 8 years, clearly show that the Indian Ocean SST variability fails to catch the recovery trend. The 20-year running mean tends to make Indian SST correlation artificially high over the recent period. Fig 2c shows also that Atlantic Ocean SST catches well the recovery after the 1980s. The statistical link with WPR is positive (fig 3d) and significant (9%, mainly between the end of the 60s and the mid-80s).

Finally, two conclusions must be drawn: (1) there is no empirical evidence of correlation stability between the selected SST indices and Sahelian rainfall at the decadal or multidecadal scales; (2) Only the eastern Mediterranean and Indian Ocean SST series show significant correlations in about 50% of years. Another striking result is that correlations with the different Oceanic basins do not occur in the same periods. Thus the anomalous wet JAS seasons observed during the 40s, 50s and 60s are mostly associated with (i) colder SST anomalies over the Indian Ocean (IND) and (ii) warmer (colder) SSTs over the TNA (TSA)

basins, which induces a northward SST anomaly gradient in the tropical Atlantic. By contrast, the drought phase following the 60s appears to be linked to (i) colder waters in the eastern Mediterranean and in the western tropical Pacific, and to (ii) Nino episodes in the central-eastern Pacific (fig. 3), compatible with the Atlantic Niño - Pacific La Niña relationship observed after the 70's by Polo et al. (2008) and Rodriguez-Fonseca et al. (2009). . It is also interesting to mention that the Indian ocean is not (is) significantly correlated with Sahelian rainfall when Sahelian rainfall is (is not) linked with Nino.

7. Linear regression and clustering

Studying the summer Sahel-ENSO teleconnection, Janicot et al. (2001) over the period 1945-1993 showed that the decadal scale SST variations weakly affect Sahel rainfall variability but that they induce an indirect effect on Sahel rainfall by enhancing the impact of the warm ENSO phases after 1980, through an increase in the fill-in of the monsoon trough and a moisture advection deficit over West Africa. Interestingly, they pointed out an adjustment in correlation after the mid-70s (1975-1980) due to the jump in SST observed for this period in the Pacific and Indian Oceans. On the basis of our results this hypothesis can be completed since no abrupt change alters the IND and Nino series used here (Fig. 2d). Moreover the SST indices document other Oceanic basins (section 2) over a larger period (1950-2008). It is therefore interesting to analyze first the summer Sahel-SST teleconnection in a more global context for quantifying the relative weights of the global (GSST) versus SST indices of regional extent in their relationship with Sahelian rainfall and African monsoon intensity. This is also supported by the fact that Pacific-Niño, Atlantic La Niña and cooling of the western Indian Ocean have, from the 70’s, an atmospheric response related to changes in the Walker circulation (Rodriguez-Fonseca et al., 2010).

For determining these weights and their time evolution, we estimate Sahel rainfall and the African monsoon intensity as depicted by the WAMI and ω indexes (section 2.3), trough linear multiple regressions after stepwise selections of 4 SST indices and cross-validation over different periods. Table 3 displays both the correlation statistics and the vectors of regression coefficients (see the legend for more details) explaining the highest part of variance. Sources of skill are found in both the quasi-global (GSST) and regional SST variability with high and significant correlations. Notice however that over the period 1950-2008, the statistical impact of GSST variability explains a smaller part of the relationship with Sahelian rainfall or the African monsoon cell (WAMI) than basin-scale variability. By contrast the GSST coefficients are higher with the vertical velocity averaged above the Sahel belt (-ω). Compared to the period 1950-1979, recent years are marked by a decrease in the teleconnection over the southern tropical Atlantic and the Indian Ocean and an increase over the Mediterranean and Nino areas and also with global warming. Overall the Mediterranean SST series registers clearly the strongest coefficients (underlined values in Table 3) with the Sahel rainfall and the African monsoon cell (WAMI).

We present now an objective cluster partition of SST series for analyzing better the structure of statistical dependencies between basin-scale indexes, using a k-means algorithm minimizing the sum, over all clusters, of the within-cluster sums of point-to-cluster-centroid distances. The procedure is applied over the period 1900-2008 on 5 regional SST indices after standardization of the series: the Mediterranean, the northern and southern tropical Atlantic, the Indian Ocean and the eastern equatorial Pacific. Several k numbers (2 to 4 classes) have been tried and we report only those with k=3 and 2 which can be estimated as the most efficient choice with respect to the number of variables and the length of the series.

First lines of table 4 display the associated cluster centroid locations from a 3-cluster partition while figure 4a shows the projection of results onto the rainfall series.

- The 'white' cluster (see white bars in fig.4 and 1st line in Tab.4) is associated with a mean SST pattern (occurrence: 34%) controlled by a cold/warm evolution in the tropical Atlantic (TNA/TSA) where warm TSA dominates, and a Nina-like growth in the Pacific, in agreement with Rodriguez-Fonseca et al. (2009). This type taking into account the inverse SST progressions in the southern Atlantic and in the equatorial eastern Pacific, will be called AP (Atlantic-Pacific). Noteworthy, this cluster is not strongly linked to Sahel rainfall variability.
- The 'blue' cluster (blue bars in fig.4 and 2nd line in Tab.4) is more frequent (40%) and clearly associated with Sahel rainfall excesses. It designates a situation where a Mediterranean warming is concomitant of warm/cold evolutions in the Atlantic with cooling over the southern Atlantic and the Indian Ocean. This cluster is therefore named MAI (Mediterranean-Atlantic-Indian).
- The 'red' cluster (bars in fig.4 and 3rd line in Tab.4) is less frequently observed (26%) but clearly occurred during the dry Sahelian phase in the 70s and 80s. It associates a Mediterranean cooling with a warming in the Indian and in the equatorial eastern Pacific (Nino-type), despite the low correlation between IND and Nino time series (section 3.3). This cluster named MIP (Mediterranean-Indian-Pacific) requires hence mechanisms linking the Indian and Pacific basins such as those illustrated in Annamalai et al. (2005) and Izumo et al. (2010). It is independent of SST variability in the Atlantic.

Let us now concentrate on the co-evolutions of Sahel rainfall (fig.4b) and cluster occurrences over successive 10-year periods between 1900 and 2008 (fig. 4c). Three points emerge: (i) the strong decadal variability affecting MAI occurrences; (ii) their negative

correlation with MIP; (iii) the resulting inverse relationship with rainfall anomalies. For example, the progressive increase/ decrease of MAI/MIP occurrence in the first part of the last century is accompanied by a long-term rise in Sahelian rainfall. Similarly, the Sahelian transition between the wet 50s and dry 70s and 80s is synchronous of a complete MAI vanishing and of a moderate MIP increase, while the partial recovery in the 90s is concomitant of the reverse. This inverse relationship involving MAI and MIP occurrences proves that the major role in the teleconnection is played by inverse thermal evolutions between the Mediterranean and Indian Ocean, although correlations between SST values averaged over these two basins are low (-0.23, -0.31 and +0.20 for the periods 1900-2008, 1950-1979 and 1980-2008). Regarding Sahelian rainfall, the opposite thermal evolution in the Mediterranean and Indian Ocean is also in good agreement with recent studies focusing on the mechanisms involved in the Indian ocean and in the Mediterranean. I.e. Bader and Latif (2009) recently showed that the warming of the Indian ocean is related to a rainfall decrease over the Sahel, while Fontaine et al. (2009) and Gaetani et al. (2010) showed that the Mediterranean warming is related to a rainfall increase over the Sahel.

The results from a partition into two clusters are displayed in fig 4b and table 4. They confirm that, situations including (excluding) opposite thermal evolution in the Mediterranean and in the Indian Ocean are (are not) associated with significant Sahelian rainfall anomalies. Additionally, the scatter-plot presented in figure 5 allows us to compare the statistical impact of inverse SST evolutions between MED and IND (x-axis) and TNA and TSA (y-axis) on the Sahelian rainy seasons since 1901. The results show clearly that MED-IND differences discriminate better rainfall anomalies than the meridional SST structure in the tropical Atlantic: more than two thirds of the rainy seasons classified as dry (wet) are concomitant of negative (positive) MED-IND differences, versus only 1/2 with TNA-TSA differences. These scores reach 16/18 (12/15) for the rainy seasons classified as very dry (very wet) versus only

10/18 (10/15) with the Atlantic dipole. This picture is in agreement with Raicich et al. (2003) results who found that a stronger than average Indian monsoon has a positive impact on the Sahelian precipitation, through the eastern Mediterranean cyclonic circulation: cold anomalies in the Indian Ocean are favourable to the monsoonal circulation over the Indian subcontinent, while warm anomalies in the Mediterranean enhance the cyclonic circulation; as a consequence the northerly flow across the Sahara is strengthened and the precipitation over the Sahel is increased.

8. Impacts of MED-IND and TNA-TSA thermal contrasts

The above statistical results show that the relationship between Sahelian rainfall and SST anomalies mostly implies the thermal variability observed over the Oceanic basins close to the African continent, especially the thermal contrasts between (i) the Mediterranean and Indian Ocean, and (ii) the northern and southern tropical Atlantic. This section is focused on these topics and on associated dynamics.

8.1 Precipitation field and atmospheric moisture flux in low levels

The analysis refers to the well documented period 1951-2000 (see section 2.1), marked by a positive phase of global warming in SST as previously shown in figure 2a, in order to focus on the region bounded by 40°S and 50°N in latitude and 60°W and 60°E in longitude (figure 6). An estimate of changes induced by linear trends in SSTs linked to global warming is also provided in the left and right panels, referring respectively to calculations before and after removing the linear trends in SSTs. It appears that such trends tend to increase the correlations but do not change neither the spatial signal at large scale, nor the pre-eminence of MED-IND variations against TNA-TSA variability. In fact, the former are synchronous of in phase rainfall anomalies over the whole Sudan-Sahel belt with areas of

inverse polarity in Brazil and central Europa (Figure 6a,b) while the latter contrasts sub-Saharan regions (i.e., Northern Africa, Sahelian belt) to the equatorial zone across the Atlantic (Guinean coast, north Brazil). They imply mechanisms of different scale: the Atlantic dipole impacts directly on the meridional structure of the rainbelt in the vicinity of the equatorial Atlantic. By contrast the larger action of MED-IND can be interpreted through the picture given by Raicich et al. (2003): cold anomalies in the Indian Ocean favour the monsoonal circulation over the Indian subcontinent, while warm anomalies in the Mediterranean strengthen the northerly flow across the Sahara, increasing precipitation over the Sahel .

The basic relationship observed with the summertime atmospheric dynamics is now investigated using a subset of the monthly NOAA-CIRES 20th Century Reanalysis over the period 1920-2008 (for the reasons listed section 2.3). We present the results from the moisture flux at 950 hPa because this field emphasizes the main elements of the monsoon circulation in low levels, in particular (i) the inter-hemispheric moisture transport along the eastern coast of Africa associated with the Indian monsoon and (ii) the African monsoon circulation between the southern-equatorial Atlantic and the Sudan-Sahel belt (Fig.7 a). Composites regarding SST differences between (i) the northern and southern tropical Atlantic basins and (ii) the eastern Mediterranean basin and the Indian Ocean are then computed. These differences are counted positive if TNA-TSA > 0 or MED-IND > 0.

The results show that both SST indices are associated with an enhancement of the African monsoon circulation on the Atlantic and the African continent. However their statistical effect on the moisture transport is clearly different. A strong TNA-TSA dipole is associated with a reinforced south-easterly flux over the western equatorial Atlantic and with an enhancement of the southwest monsoon over the Sahelian belt (figure 7b). By contrast, a positive MED-IND index reinforces the northerlies and southerlies over the Atlantic (Figure 7c) and therefore the interhemispheric moisture flux convergence. In addition the

northeasterly transport from the eastern Mediterranean and the southwest transport from the eastern equatorial Atlantic (i.e., the monsoon flow) are both strengthened: in agreement with the empirical and numerical results of Rowell (2003), Fontaine et al. (2009) and Gaetani et al. (2010) this can produce an anomalous poleward ITCZ-extension.

8.2 Atmospheric circulation

We investigate now the atmospheric circulation in northern summer on the period 1920-2008 from (i) the vertical atmospheric motion ($-\omega$ in $Pa.s^{-1}$) and (ii) the divergent part (irrotational) of the horizontal wind ($m.s^{-1}$) which is proportional to the gradient of the velocity potential ($m^2.s^{-1}$). The use of the divergent horizontal wind removes any continuity problem when the circulation is averaged along the zonal and meridional directions. Notice also that computations have been made on the global field to avoid any bias.

The meridional component of this circulation, averaged over the African longitudes (20°W-40°E) is displayed in figure 8a. It portrays the meridional overturning in the region, associated with the Hadley circulation. The monsoonal circulation in low-levels is marked here by the shift of air ascents in low troposphere over Sudan-Sahel and by a small northerly component in mid-levels, at the altitude of the African Easterly Jet (700-600 hPa). Since the meridional plane captures well these basic features, it is interesting to concentrate on changes induced by variations in MED-IND and TNA-TSA contrasts.

The MED-IND composite (figure 8b) exhibits clear ascents in low and mid levels around 40°N in relation to the warming of the Mediterranean basin. Southerly anomalies are noticed in all the troposphere between 45°N and 60°N while northerly departures prevail above 500 hPa over the 20°N-40°N latitudes. This denotes a region of divergence anomaly in upper levels in the northern subtropics (35°N-40°N). Southward, above the monsoon region, a general descent from mid-levels towards the surface is evidenced above 10°N-18°N and

associated with rising motion above the Saharan thermal lows, i.e., at the latitude of the northern Tropic. Above 500 hPa where moist convection develops, upward anomalies are present over the Sahelian belt.

The TNA-TSA composite (figure 8c) is very different. The significant signals are mainly located in the southern hemisphere. Over Northern Africa a general subsidence departure above 5°N is evidenced in the whole troposphere whereas ascents prevail in mid and high levels south of 10°S. These opposed vertical anomalies are in agreement with the rainfall contrasts, displayed in figure 6c,d, between sub-Saharan regions and the Guinea coast. Notice that there is no signal above the Sahel in high troposheric levels where moist convection is observed.

The east-west circulation has been averaged between 15°N and 20°N (figure 9). Mean values (figure 9a) point to (i) the summertime Indian east-west cell marked by upward motions over the western part of the Ocean (east of 45°E) and descents over northern Africa (west of 45°E); (ii) the thermal contrast between the cool eastern Atlantic marked by air subsidence and the hot Saharan in the vicinity of the thermal low westward to 5°W marked by atmospheric heating and ascents.

The MED-IND composite (fig 9b) firstly shows that ascents in the lower troposphere decrease above the central Sahel, while descents in upper levels are weakened on the eastern Atlantic and above the western (20°W-5°W) and eastern Sahel (15°E-30°E). Then, an area of low level subsidence anomaly by 30°E-40°E, i.e., associated with the relative Indian cooling, weakens the normal uplifts shown in figure 9a. Finally, the Tropical easterly Jet is reinforced by the upper branch of the zonal overturning between the 0° meridian and 20°E. This is in agreement with a reinforcement of deep convection processes over central-eastern Sudan-Sahel, since these processes, following Chen (2005), are linked to the dynamics of the midtropospheric divergent center maintained by the east-west circulation and the Saharan

thermal-low.

The TNA-TSA composite exhibits few significant upward departures above the northern tropical Atlantic as the thermal response of the atmosphere to the relative surface warming. By contrast, no significant signal above Africa (20°W-40°E) can be noticed, except a divergence area at 600 hPa in the Western Sahel and an easterly wind component between 25°E and 45°E in high troposphere.

9. Discussion and conclusion

The objective of this study was to revisit the question of the July-September SST-African rainfall teleconnection variability in separating basin-scale variability from the direct impact of the quasi-global thermal evolution observed since 1900, regardless of its natural or anthropogenic origin. Using statistical methods such as linear correlation, linear multiple regression, composite and cluster analyses, the results confirmed that the relationship is rather linear without significant differences between African longitudes but concerns more the Sahelian belt than the subequatorial zone. Interestingly, the SST-Sahel teleconnection appears more often significant with the Mediterranean index (positive correlation) and with the Indian Ocean (negative correlation) all along the period in about 50% of years. By contrast, significant correlations observed with SSTs in other basins are less frequent : only in the 50s-70s, during the negative trend in Sahelian rainfall, for the southern Atlantic basin and the meridional Atlantic dipole; Only during the anomalous 70s-80s dry period for the western Pacific region and since the end of the 60s for the Nino area.

Analyzing the relationship in a more global context through both regional rainfall estimates and atmospheric indices representative of the African monsoon intensity (WAMI and -ω), we showed that the quasi-global warming (GSST) explains a small part of the relationship except with vertical ascents above the African Sahel. The Tropical Atlantic and

equatorial Pacific signals impact also moderately. Overall, the dominant statistical linkage, both in terms of intensity and time stability, is found with the Mediterranean basin and with the Indian Ocean. In the recent period, marked by a moderate rainfall recovery, the teleconnection decreases in the southern tropical Atlantic and Indian Ocean and increases with GSST and over the Mediterranean and Nino areas.

Additional regression and cluster analyses allowed us to focus more on the SST signals observed in the Oceanic basins close to the African continent. We showed that, with a statistical point of view, the TNA-TSA differences (the Atlantic dipole) are less efficient than the MED-IND differences to discriminate correctly the Sahelian rainfall anomalies: wetter (dryer) rainy seasons are primarily associated with warmer (colder) anomalies in the Mediterranean, and colder (warmer) anomalies in the Indian Ocean. Indeed more than two thirds of the rainy seasons classified as dry (wet) are concomitant of negative (positive) MED-IND differences; these scores reach 16/18 (12/15) for the rainy seasons classified as very dry (very wet).

The connection observed with continental precipitation over a larger domain (60°W-60°E) confirmed this feature and showed that removing linear trends in the SST series decreases correlation values without changing drastically the spatial patterns. The statistical effects of SST variability on the 950 hPa moisture flux field and overturning circulation along the meridional and zonal planes have been also depicted. The results obtained can be summarized as follows.

Positive TNA-TSA differences tend to generate opposite rainfall anomalies along the meridional plane, i.e., above normal rainfall in sub-Saharan regions and below normal amounts across the equatorial Atlantic (Guinean coast, north Brazil). A northward SST gradient in the tropical Atlantic is mainly associated with: (i) significant upward atmospheric

motion, a thermal response of the atmosphere to the surface warming in the northern basin; (ii) a reinforcement of the moisture transport from the south-east over the western equatorial Atlantic and the Sahelian belt; (iii) a general subsidence anomaly above 5°N over Africa in the whole troposphere. The two last points are coherent with the dipolar rainfall response over the Sahelian and Guinean regions.

By contrast, the positive MED-IND differences are concomitant with rainfall excess over the whole Sudan-Sahel belt and with rainfall drying in Brazil and central Europe. This is associated with an enhancement of both the north-easterly moisture transport from the eastern Mediterranean and the monsoon south-westerly moisture transport from the eastern equatorial Atlantic by the monsoon flow. Such rainfall and atmospheric patterns reproduce well several elements of the teleconnection observed between the Mediterranean and the African monsoon (Rowell, 2003; Raicich et al., 2003; Fontaine et al., 2010). However, four additional signals have been reported in the monsoon region: (i) a subsidence departure from mid-levels above 10°N-18°N associated with air ascents above the Saharan thermal lows; (ii) upward anomalies on the western and eastern Sahel reinforcing the normal atmospheric ascents linked to deep convection in upper levels; (iii) a low-level subsidence anomaly by 30°E-40°E in agreement with the Indian cooling weakening the normal uplifts; (iv) a reinforcement of the Tropical easterly Jet over 0°-20°E.

Acknowledgements

The authors are grateful to the University of East Anglia, Global Precipitation Climatology Centre (GPCC), the National Oceanic and Atmospheric Administration, the National Center for Atmospheric Research and National Centers for Environmental Prediction for providing most of the data presented in section 2. The study was supported by the TELEMEDAF (Italian CNR / French CNRS joint project) and by the Global change and Ecosystems

programme EU Integrated project: African Monsoon Multidisciplinary Analysis (AMMA) and the French component of AMMA. Based on a French initiative, AMMA was built by an international scientific group and has been funded by a large number of agencies, especially from France, UK, US and Africa. It has been the beneficiary of a major financial contribution from the European Community's Sixth Framework Research Programme. Calculations were performed using HPC resources from DSI-CCUB (Université de Bourgogne).

References

Annamalai, H., S.-P. Xie, J.P. McCreary, and R. Murtugudde, 2005: Impact of Indian Ocean sea surface temperature on developing El Niño. J. Climate, 18, 302–319.

Bader and Latif, 2009: The 1983 drought in the West Sahel: a case study. Clim. Dyn. doi: 10.1007/s00382-009-0700-y

Bader, J., and M. Latif, 2003: The impact of decadal-scale Indian Ocean sea surface temperature anomalies on Sahelian rainfall and the North Atlantic Oscillation. Geophys. Res. Lett., 30, 2169, doi:10.1029/2003GL018426.

Beck, C., J. Grieser and B. Rudolf, 2005: A New Monthly Precipitation Climatology for the Global Land Areas for the Period 1951 to 2000. DWD, Klimastatusbericht 2004, 181-190. Biasutti M., Held I. M, Sobel A. H., Giannini A., 2008, SST Forcings and Sahel Rainfall Variability in Simulations of the Twentieth and Twenty-First Centuries. J. Climate, 21, 3471-3486. DOI: 10.1175/2007JCLI1896.1

Biasutti, M., and A. Giannini, 2006: Robust Sahel drying in response to late 20th century forcings. Geophys. Res. Lett., 33, L11706, doi:10.1029/ 2006GRL026067.

Bell, M. A., and P. J. Lamb, 2006, Integration of weather system variability to multidecadal regional climate change: The West African Sudan-Sahel zone, 1951-98. *J. Climate,* **19**, 5343-5365.

Caminade C and Terray L, 2010, Twentieth century Sahel rainfall variability as simulated by the ARPEGE AGCM, and future changes, Climate Dynamics, 11, 75-94, DOI: 10.1007/s00382-009-0545-4.

Charney, J., W.J. Quirk, S.-H. Chow, and J. Kornfield, 1977: A comparative study of the effects of albedo change on drought in semi-arid regions. *J. Atmos. Sci.*, **34**, 1366-1385, doi:10.1175/1520-0469(1977)034<1366:ACSOTE>2.0.CO;2.

Chen T-C, 2005, Maintenance of the Midtropospheric North African Summer Circulation: Saharan High and African Easterly Jet, Journal of Climate, 18, 2943-2962.

Compo,G.P. , J.S. Whitaker , and P.D. Sardeshmukh, 2006: Feasibility of a 100 year reanalysis using only surface pressure data, Bull. Amer. Met. Soc., 87, 175-190.

Delworth TL, Manabe S, Stouffer RJ (1993) Interdecadal variations of the thermohaline circulation in a coupled Ocean–atmosphere model. J Clim 6:1993–2011.

Folland, C. K., T. N. Palmer, and D. E. Parher, Sahel rainfall and worldwide sea temperatures, Nature, 320, 602–607, 1986.

Fontaine B., J. Garcia-Serrano, P. Roucou, B. Rodriguez-Fonseca, T. Losada, F. Chauvin, S. Gervois, S. Sivarajan, P. Ruti, S. Janicot (2009): Impacts of Warm and Cold situations in the Mediterranean Basins on the West African monsoon: observed connection patterns (1979-2006) and climate simulations. Climate Dynamics, ISSN0930-7575 (Print) 1432-0894 (Online), published online 11 June 2009, DOI 10.1007/s00382-009-0599-3.

Gaetani, M., B. Fontaine, P. Roucou, and M. Baldi (2010), Influence of the Mediterranean Sea on the West African Monsoon: intraseasonal variability in numerical simulations, J. Geophys. Res., doi:10.1029/2010JD014436, accepted 24 September 2010, in press.

Giannini, A., R. Saravanan, and P. Chang, 2003: Oceanic forcing of Sahel rainfall on interannual to interdecadal time scales. Science, 302, 1027–1030.

Goldenberg, S. B.; et al. (2001). "The recent increase in Atlantic hurricane activity: Causes and implications". Science 293: 474–479. doi:10.1126/science.1060040.

Hastenrath, S. and P. J. Lamb, 1977, Climatic Atlas of the Tropical Atlantic and Eastern Pacific Oceans, 97 charts, Univ. of Wisconsin Press, Madison, Wisc..

Hastenrath, S. and Polzin D., 2010, Long-term variations of circulation in the tropical Atlantic sector and Sahel rainfall, Int. Journal of Climatology, 10.1002/joc.2116.

Hodson DLR, Sutton RT, Cassou C, Keenlyside N, Okumura Y and Zhou T., 2010, Climate impacts of recent multidecadal changes in Atlantic Ocean Sea Surface Temperature: a multimodel comparison, Climate Dynamics, Volume 34, Numbers 7-8 / june 2010, 1041-1058, DOI 10.1007/s00382-009-0571-2

Izumo T., Vialard J., Lengaigne M, de Boyer Montegut C., Behera S-K., Luo JJ, Cravatte S, Masson S and Yamagata T., 2010, Influence of the state of the Indian Ocean Dipole on the following year's El Niño, published online: 21 February 2010, doi:10.1038/ngeo760.

Janicot S.,, Trzaska S. and Poccard I.,, 2001: "Summer Sahel – ENSO teleconnection and decadal time scale SST variations", Climate Dynamics, 18, 303-320

Janowiak, E. J. (1988) An investigation of interannual rainfall variability in Africa. *J. Climate* 1, 240-255.

Joly M. and A. Voldoire, 2009, Influence of ENSO on the West African monsoon: temporal aspects and atmospheric processes Journal of Climate, 22, 3193–3210

Joly M., and A. Voldoire, 2010: Role of the Gulf of Guinea in the inter-annual variability of the West African monsoon: what do we learn from CMIP3 coupled simulations? Int. J. Climatol., doi: 10.1002/joc.2026

Kim K-M, Lau W-K, Sud YC and Walker GK, 2010, Influence of aerosol-radiative forcings on the diurnal and seasonal cycles of rainfall over West Africa and Eastern Atlantic Ocean using GCM simulations, Climate Dynamics, 11, 115 – 126, doi:10.1007/s00382-010-0750-1

Lamb, P. J., 1978, Large-scale tropical Atlantic surface circulation patterns associated with sub-saharan weather anomalies, Tellus, 30, 240– 251.

Losada, T., B. Rodriguez-Fonseca, S. Janicot, S. Gervois, F. Chauvin, and P. Ruti, 2009: A multimodel approach to the Atlantic equatorial mode. Impact on the West African monsoon. Clim. Dyn., doi: 10.1007/s00382-009-0625-5

Lough, J. M., 1986, Tropical Atlantic sea surface temperature and rainfall variations in subsaharan Africa month, Mon. Weather Rev., 114, 561–570.

Mitchell TD, Carter TR, Jones PD, Hulme M, New M. 2004. A comprehensive set of high-resolution grids of monthly climate for Europe and the globe: the observed record (1901-2000) and 16 scenarios (2001-2100). Tyndall Working Paper 55, Tyndall Centre, UEA, Norwich, UK. http://www.tyndall.ac.uk/

Mohino, E., S. Janicot, and J. Bader, 2010: Sahelian rainfall and decadal to multidecadal SST variability. Clim. Dyn., doi: 10.1007/s00382-010-0867-2

New M, Lister D, Hulme M, Makin I, 2002: A high-resolution data set of surface climate over global land areas. Climate Research 21: 1–25

Nicholson, S. E., 1979, Revised rainfall series for the West African subtropics. *Mon. Wea. Rev.,* **107,** 620-623.

Nicholson, S. E., and R. S. Nyenzi, 1990, Temporal and spatial variability of SSTs in tropical Atlantic and Indian Oceans, Meteorol. Atmos. Phys., 42, 1 – 17

Palmer, T. N., 1986,The influence of the Atlantic, Pacific and Indian Oceans on Sahel rainfall, Nature, 322, 251– 253.

Polyakov I.V., Alexeev V.A. Bhatt U.S., Polyakova E.I. and Zhang X., 2010, North Atlantic warming: patterns of long-term trend and multidecadal variability, Clim Dyn (2010) 34:439–457, DOI 10.1007/s00382-008-0522-3.

Raicich, F., N. Pinardi and A. Navarra, 2003,Teleconnections between Indian monsoon and Sahel rainfall and the Mediterranean. Int. J. Climatol. 23, 173–186.

Rodríguez de Fonseca B., S. Janicot, T. Losada, E Mohino, M. Joly, A. Voldoire, B. Fontaine, J. Bader, C. Caminade, I. Polo, J. Garcia-Serrano, F. Chauvin, P. Ruti, S. Gervois, P. Roucou, 2010, Interanual and decadal SST forced responses of the West African monsoon, accepted in Atmospheric Science Letters.

Rodríguez-Fonseca, B., I. Polo, J. García-Serrano, T. Losada, E. Mohino, C. R. Mechoso, and F. Kucharski, 2009: Are Atlantic Niños enhancing Pacific ENSO events in recent decades? Geophys. Res. Lett., 36, L20705, doi:10.1029/2009GL040048.

Rowell D.P., 2003, The Impact of Mediterranean SSTs on the Sahelian Rainfall Season. J. Clim., 16, 849-862

Saha, S. and Coauthors, 2006: The NCEP Climate Forecast System. J. Climate, 19, 3483-3517.

Smith, T.M., R.W. Reynolds, Thomas C. Peterson, and Jay Lawrimore 2007, Improvements to NOAA's Historical Merged Land-Ocean Surface Temperature Analysis (1880-2006). In press. Journal of Climate (ERSSTV3)

Stott, P. A., S. F. B. Tett, G. S. Jones, M. R. Allen, J. F. B. Mitchell, and G. J. Jenkins, 2000: External control of 20th century temperature by natural and anthropogenic forcings. Science, 290, 2133–2136.

Walker and Rowntree, 1977, J. Walker and P.R. Rowntree, The effect of soil moisture on circulation and rainfall in a topical model. *Q. J. R. Met. Soc.* **103**, 29–46.

Ward, M. N., C. K. Folland, K. Maskell, D. Rowell, and A. Colman, 1990, Understanding and predicting seasonal rainfall in subSaharan Africa, Trop. Meteorol. Res. Programme Rep. Ser., 36, 157–161.

Ward MN., 1998, Diagnosis and short-lead time prediction of summer rainfall in tropical North Africa at interannual and multidecadal timescales. *Journal of Climate* **11**: 3167–3191.

Xue, Y., R.W.A. Hutjes, R.J. Harding, M. Claussen, S. Prince, E. F. Lambin, S. J. Allen, P. Dirmeyer, T. Oki, 2004, The Sahelian Climate (Chapter A5) in Vegetation, Water, Humans and the Climate, Eds, P. Kabat, M. Claussen, P. A. Dirmeyer, J. H. Gash, L. B. Deguenni, M. Meybeck, R. A. Pielke, sr, C. J. Vorosmarty, R. W. A. Hutjes, and S. Lutkemeier. Springer-Verlag, Berlin Heidelberg, P59-77.

Zeng, N., Neelin, J. D., Lau, K. M. & Tucker, C. J. 1999 Enhancements of interdecadal climate variability in the Sahel by vegetation interaction. *Science* 286, 1537–1540.

Zhang, R.; Delworth, T. L., 2006, Impact of Atlantic multidecadal oscillations on India/Sahel rainfall and Atlantic hurricanes". Geophys. Res. Lett. 33: L17712. doi:10.1029/2006GL026267.

TABLES

	Western region		Central region		Eastern region	
	SAH	*GUI*	SAH	*GUI*	SAH	*GUI*
GSST	-52*				-35*	
AMO						
WMED	+44**		+40**			*+35**
EMED	+48**		+54**		+43**	*+31**
TNA						
TSA	-35*	*+35***	-42**	*+35***	-35*	*-34**
IND	-53**	*-29**	-45**		-37*	
NINO	-30*		-29*		-34**	*-40***

Table 1: Significant correlation coefficients (*100) between SST indexes and CRU rainfall averaged in the Sahelian (SAH: 10°N-20°N) and Guinean (GUI: 5°N-9.5°N) belts computed over the period 1950-2002 and in the western (15W-0°), central (0°-15°E) and eastern (15°E-30°E) longitudes.. *,** for significance at p=0.05 and 0. 01.

TNA	< -0.5	> +0.5
SAH+	26%	22%
SAH-	28%	25%

MED	< -0.5	> +0.5
SAH+	13%	**38%**
SAH-	**38%**	12%

TSA	< -0.5	> +0.5
SAH+	25%	22%
SAH-	22%	**32%**

IND	< -0.5	> +0.5
SAH+	**40%**	14%
SAH-	16%	**30%**

DIP	< -0.5	> +0.5
SAH+	27%	27%
SAH-	24%	22%

NINO	< -0.5	> +0.5
SAH+	**31%**	18%
SAH-	19%	**32%**

Table 2: Contingency tables between the sign of the Sahel rainfall index (SAH+, SAH-) and values of SST indexes below -0.5 std (cold situations) or above +0.5 std (warm situations) in selected basins: the tropical northern Atlantic (TNA), the Mediterranean (MED), the tropical southern Atlantic (TSA), the Atlantic dipole (DIP=TNA-TSA), the equatorial eastern Pacific (NINO) and the Indian Ocean (IND). The values are expressed in percentages of occurrences (the sum of four percentages for each Ocean basin is 100%. Values > 30% in bold. Period 1900-2008.

	R Rcv Racv	GSST	TSA	MED	IND	NINO area
SAHEL 50-08	+84 +79 +59	-34	-22	**+54**	-37	
50-79	+91 +88 +72		-44	**+45**	-37	-15
80-08	+81 +67 +32	+03		**+65**	-17	-40
WAMI 50-08	+72 +66 +39	-23	-34	**+38**	-32	
50-79	+74 +64 +28	+19	-38	**+42**	-31	
80-08	+89 +84 +65	+38	-24	**+48**		-39
- ω 50-08	+67 +60 +30	**-40**	-26	+30	-23	
50-79	+66 +48 +06	+19	-31	**+49**	-14	
80-08	+85 +77 +51	**+49**	-15	+32		-44

Table 3: Linear multiple regression (LMR) estimating the July-September Sahel rainfall amounts and two African monsoon descriptors (WAMI and – ω, see section 2) after stepwise selections of the best 4 SST indices (columns 3-7). All the series have been standardized before applying the procedure ensuring easier comparisons.
column 2: Total correlation (R), correlation after cross-validation (Rcv) and adjusted correlation after cross-validation (Racv).
columns 3-7: the vector of regression coefficients (*100) in the linear model (highest value in bold). Three periods are considered (column 1): 1950-2008, 1950-1979 and 1980-2008.

Clusters and % occurrence	MED	TNA	TSA	IND	Nino area
3-cluster partition with 5 SST series (see fig. 3a)					
White (34%)	+0.02	-0.40	**+0.70**	-0.06	**-0.73**
Blue (40%)	**+0.60**	+0.33	**-0.60**	**-0.61**	+0.12
Red (26%)	**-0.97**	+0.01	+0.02	**+1.03**	**+0.78**
2-cluster partition with 5 SST series (see fig. 3b)					
Blue	**+0.56**	+0.26	-0.49	**-0.61**	-0.10
Red	**-0.51**	-0.24	+0.45	**+0.56**	+0.09

Table 4: Cluster centroid locations (and percentages of occurrence) of partitions in 3 and 2 clusters based on squared Euclidean distances between the standardized SST time series over the period 1900-2008 : MED (Mediterranean); TNA, TSA (northern and southern tropical

Atlantic); IND (Indian Ocean) and the Nino (eastern equatorial Pacific). The k-means algorithm has been repeated 100 times, each time with a new set of initial centroids, ensuring that the convergence criterion is met (the assignment remains the same). Values higher than |0.5| in bold.

Figures

Figure 1. Temporal correlation coefficients between the Sahel rainfall index and the quasi-global SST field in July-September for different sub-periods : a) 1900-1949; b) 1950-1970; c) 1971-1990; d) 1991-2008. Values above |0.3| (~10% of common variance) are displayed in blue (red) contours for the negative (positive) values with a 0.2 interval; shadings superimposed when they exceed |0.5|. The green boxes in panel a) indicate the Oceanic regions used for defining the SST regional indices presented in section 5.

Figure 2. Time evolution of the July-September standardized time series of Sahel rainfall (bars) on the period 1900-2008 and of a few selected low frequency SST anomaly indices (superimposed curves) over the period 1860-2009).

a) Atlantic Multidecadal Oscillation (AMO, dashed curve) and near Global SSTs (GSST, solid): details in sections 4 and 5.

b) Western (dashed curve) and Eastern (solid) Mediterranean SSTs: WMED:[32°N-44°N; 6°W-15°E]; EMED [32°N-44°N; 15°E-36°E].

c) Tropical Northern (dashed curve) and Southern (solid) Atlantic SSTs: TNA [5°N-24°N; 50°W-15°W], TSA [20°S-0°; 30°W-10°E] along with the TNA-TSA difference (dashed dotted with circles).

d) Indian (IND, dashed curve), Nino 3.4 (solid) and West Pacific Region WPR (dashed dotted with circles) SSTs: IND [24°S-24°N; 35°E-90°E]; Nino3.4 [5°S-5°N; 170°W-120°W]; WPR [20°N-20°S; 100°E-160°E].

In panels b-d, quasi-decadal / multi-decadal SST signal have been isolated from higher frequencies using a zero-phase forward and reverse digital filtering (Murakami,1979) for eliminating time variability < 8 year at each grid-point of the weighted SST anomaly field.

Figure 3. Correlation coefficients computed on 20-year running windows between the Sahel rainfall index and the SST indexes displayed in figure 2.
The x-axis is labelled with the first year of the 20-y ear period, so 1900 means 1900-1919. Symbols are superimposed when the values are significant regarding significance tests based on permutation resamples drawn at random from the original data and Monte Carlo procedure. a,b,c,d as in fig.1. The titles indicate the relative percentage of significant values on the period. 1900-2008.

Figure 4. Time projections of the Kmeans results displayed in Table 3 onto the standardized Sahel rainfall series at an interannual timestep (a,d) and co-variation with Sahel rainfall in mm/month over 10-year sub-periods (b,c) between 1900 and 2008: AP (white), MAI (blue) and MIP (red).

Figure 5. Scatter-plot of summertime (JAS) Sahelian rainfall as a function of the differences computed between the MED and IND (x-axis) and TNA and TSA (y-axis) standardized time series. ‘W’ (‘D’) denote the wettest (driest) rainfall anomalies, i.e., those exceeding 1 sd in absolute value, while ‘+’ and ‘–‘ refer to other positive (negative) anomalies. Period. 1900-2008.

Figure 6. Correlation coefficients with the rainfall field in July-September using the Vasclimo SST data (period 1951-2000). Panels a,b (c,d) refer to the results obtained with SST differences defined between the eastern Mediterranean and Indian basins (the northern and southern tropical Atlantic) with (left) and without(right) linear trends. Values below |0.25| are not displayed.

Figure 7. July-September moisture flux at 950 hPa over the period 1920-2008. (a) mean values; (b) significant differences between the northern and southern tropical Atlantic basins; (c) significant differences between the eastern Mediterranean basin and the Indian Ocean. The statistical significance has been estimated on the zonal and meridional components through a Student t-test contrasting the 20 highest and the 20 lowest seasonal differences versus all the remainders.

Figure 8. July-September atmospheric circulation (divergent wind, $-\omega$) along a meridional-vertical plane averaged between 20°W and 40°E over the period 1920-2008. (a) Mean values; (b) MED-IND composite relative to SST differences between the eastern Mediterranean basin and the Indian Ocean (c) TNA-TSA composite relative to SST differences between the northern and southern tropical Atlantic basins. In panels (b,c) only the significant values are displayed. The statistical significance has been estimated on the vertical and meridional components through a Student t-test contrasting the 20 highest and the 20 lowest seasonal differences versus all the remainders.

Figure 9. As figure 8 but for the July-September atmospheric circulation along a zonal-vertical plane averaged between 15°N and 20°N.

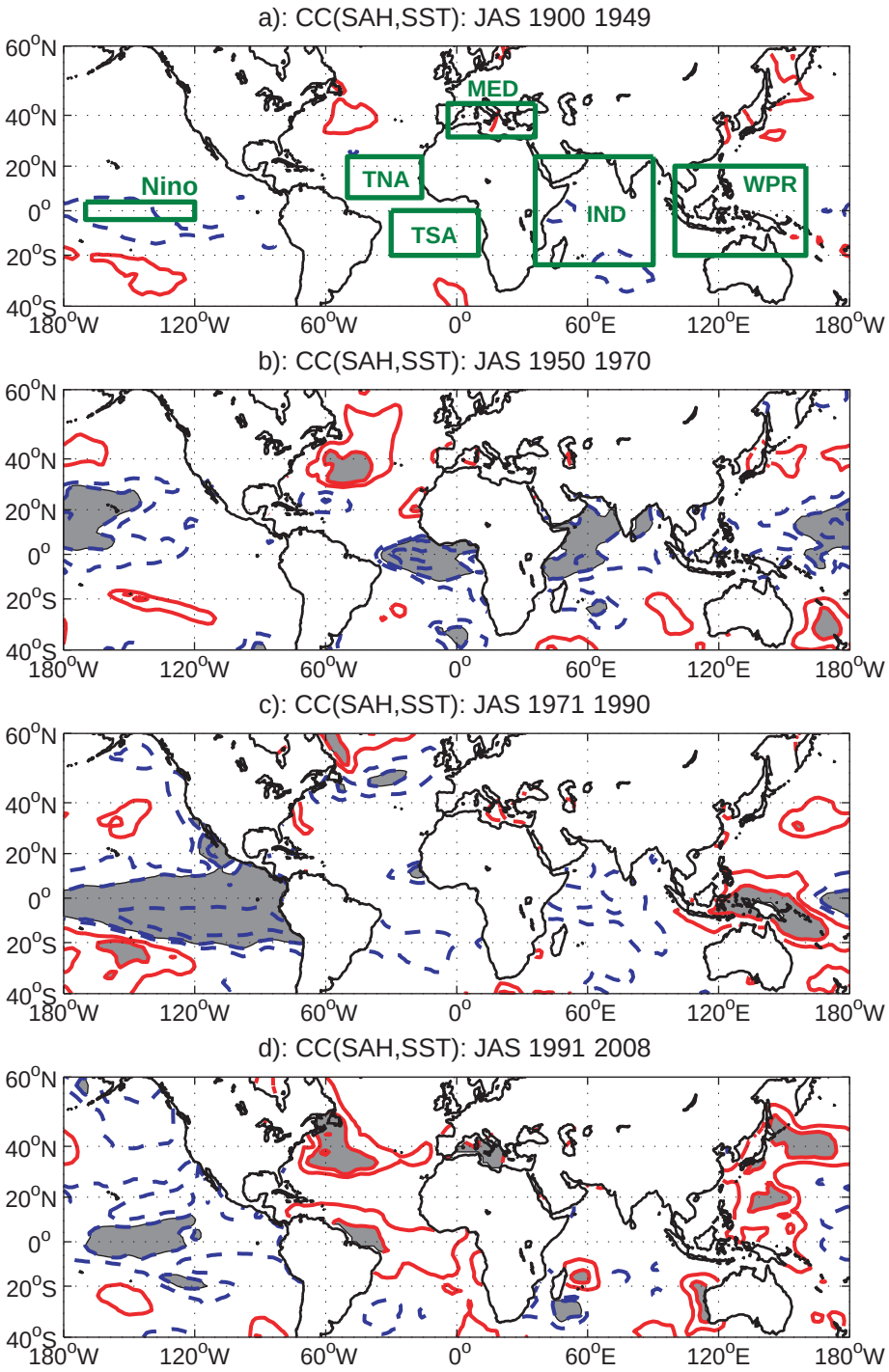
a): CC(SAH,SST): JAS 1900 1949
b): CC(SAH,SST): JAS 1950 1970
c): CC(SAH,SST): JAS 1971 1990
d): CC(SAH,SST): JAS 1991 2008
Nino
TNA
TSA
MED
IND
WPR
60°N
40°N
20°N
0°
20°S
40°S
180°W
120°W
60°W
0°
60°E
120°E
180°W

Figure 1. Temporal correlation coefficients between the Sahel rainfall index and the quasi-global SST field in July-September for different sub-periods: a) 1900-1949; b) 1950-1970; c) 1971-1990; d) 1991-2008. Values above |0.3| (~10% of common variance) are displayed in blue (red) contours for the negative (positive) values and with a 0.2 interval and shadings superimposed when they exceed |0.5|. The green boxes in panel a indicate the Oceanic regions used for defining the SST regional indices presented in section 5.

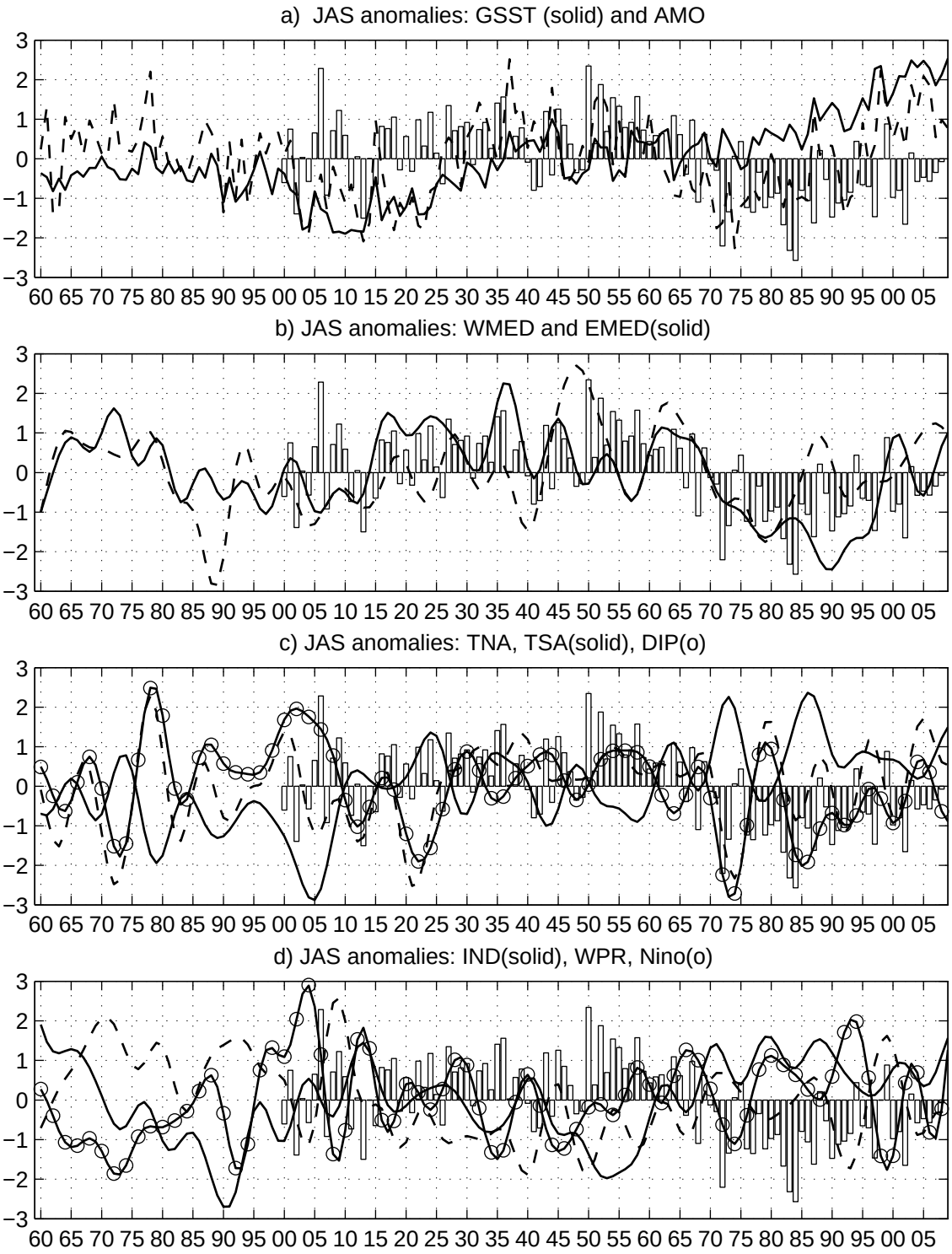

Figure 2. Time evolution of the July-September standardized time series of Sahel rainfall (bars) on the period 1900-2008 and of a few selected low frequency SST anomaly indices (superimposed curves) over the period 1860-2009).

a) Atlantic Multidecadal Oscillation (AMO, dashed curve) and near Global SSTs (GSST, solid): details in sections 4 and 5.

b) Western (dashed curve) and Eastern (solid) Mediterranean SSTs: WMED:[32°N-44°N; 6°W-15°E]; EMED [32°N-44°N; 15°E-36°E].

c) Tropical Northern (dashed curve) and Southern (solid) Atlantic SSTs: TNA [5°N-24°N; 50°W-15°W], TSA [20°S-0°; 30°W-10°E] along with the TNA-TSA difference (dashed dotted with circles).
d) Indian (IND, dashed curve), Nino 3.4 (solid) and West Pacific Region WPR (dashed dotted with circles) SSTs: IND [24°S-24°N; 35°E-90°E]; Nino3.4 [5°S-5°N; 170°W-120°W]; WPR [20°N-20°S; 100°E-160°E].
In panels b-d, quasi-decadal / multi-decadal SST signal have been isolated from higher frequencies using a zero-phase forward and reverse digital filtering (Murakami,1979) for eliminating time variability < 8 year at each grid-point of the weighted SST anomaly field.

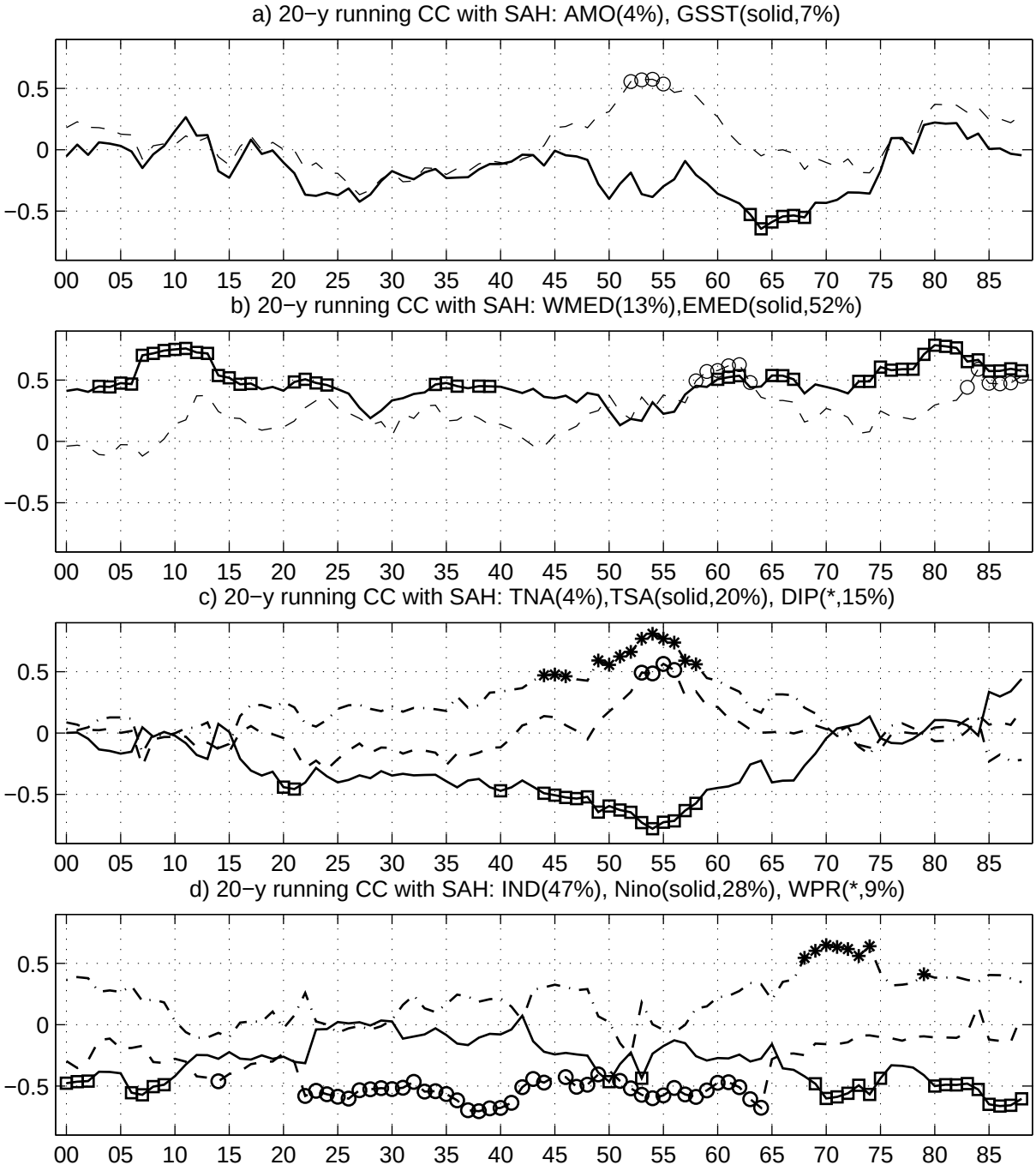

Figure 3. Correlation coefficients computed on 20-year running windows between the Sahel rainfall index and the SST indexes displayed in figure 2.

The x-axis is labelled with the first year of the 20-y ear period, so 1900 means 1900-1919. Symbols are superimposed when the values are significant regarding significance tests based on permutation resamples drawn at random from the original data and Monte Carlo procedure. a,b,c,d as in fig.1. The titles indicate the relative percentage of significant values on the period. 1900-2008.

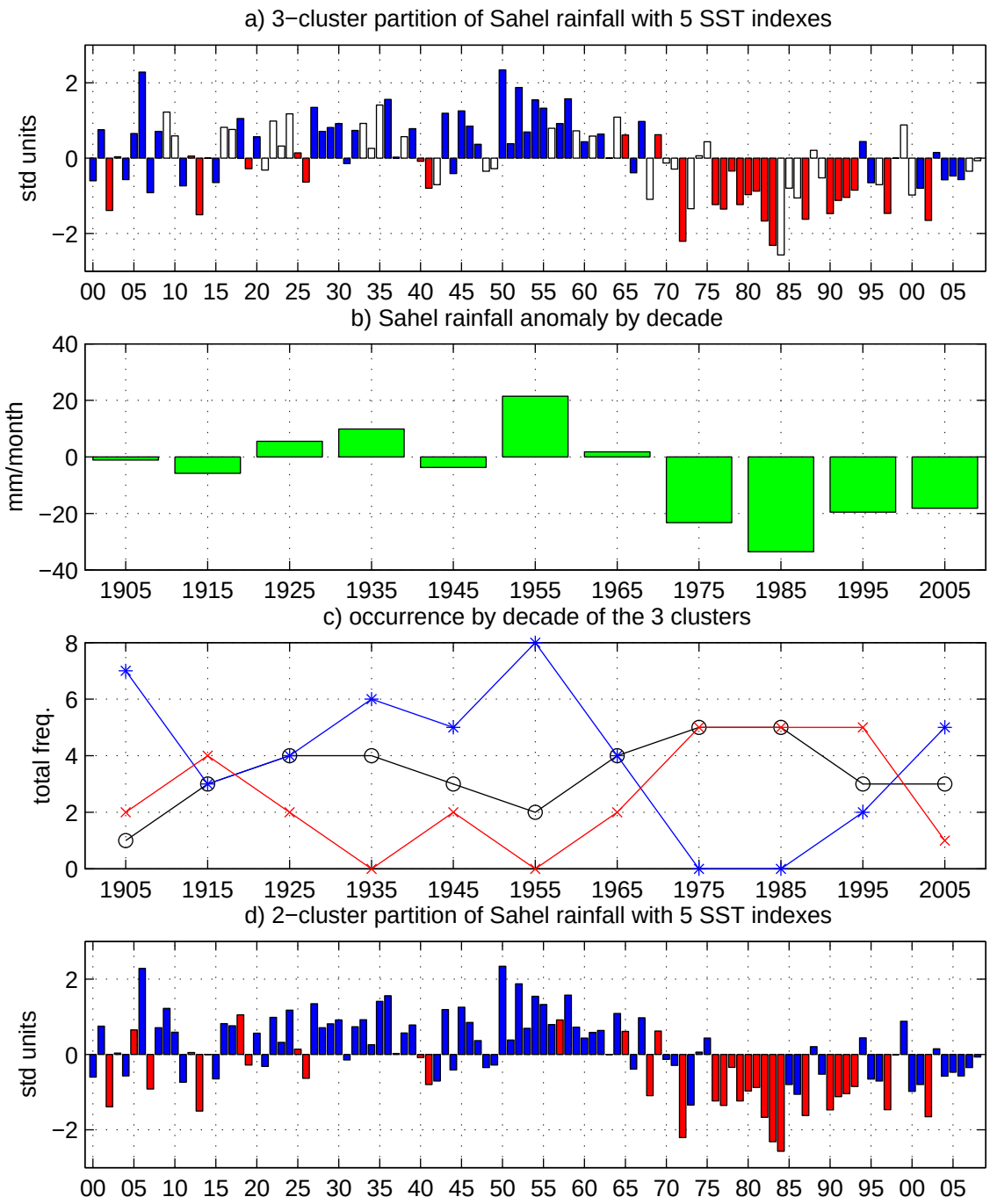

Figure 4. Time projections of the Kmeans results displayed in Table 3 onto the standardized Sahel rainfall series at an interannual timestep (a,d) and co-variation with Sahel rainfall in mm/month over 10-year sub-periods (b,c) between 1900 and 2008: AP (white), MAI (blue) and MIP (red).

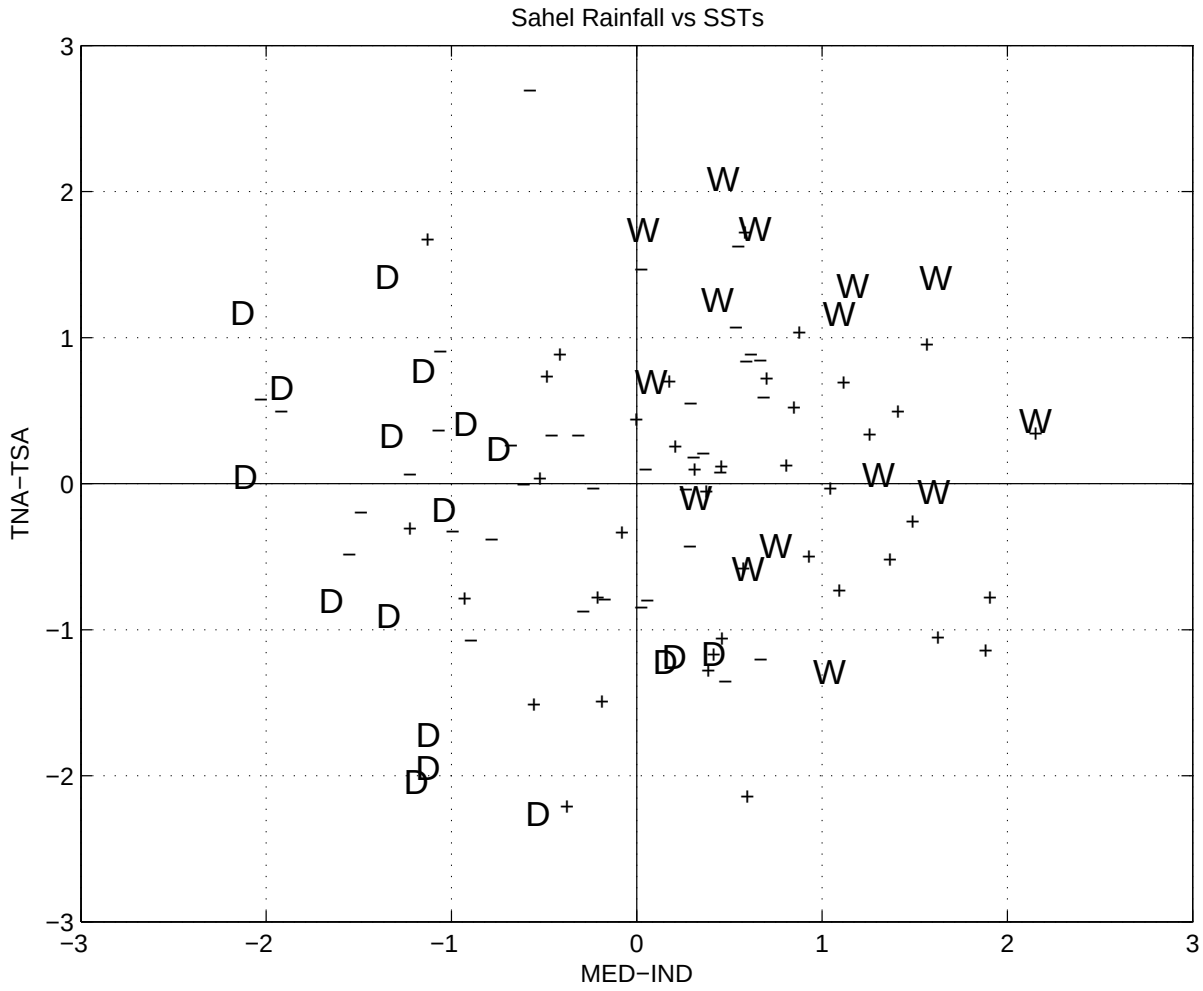

Figure 5. Scatter-plot of summertime (JAS) Sahelian rainfall as a function of the differences computed between the MED and IND (x-axis) and TNA and TSA (y-axis) standardized time series. 'W' ('D') denote the wettest (driest) rainfall anomalies, i.e., those exceeding 1 sd in absolute value, while '+' and '–' refer to other positive (negative) anomalies. Period. 1900-2008.

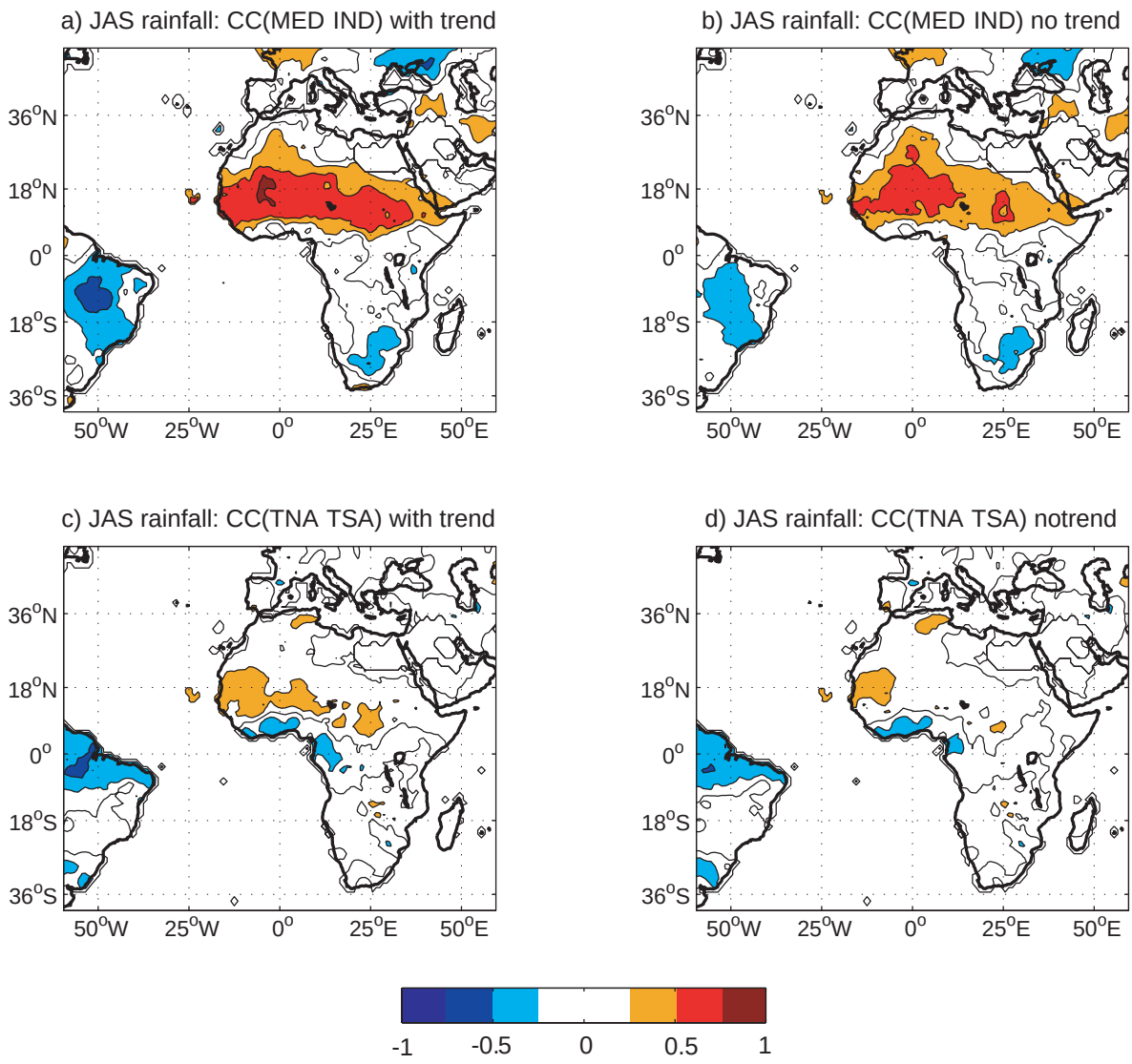

Figure 6. Correlation coefficients with the rainfall field in July-September using the Vasclimo SST data (period 1951-2000). Panels a,b (c,d) refer to the results obtained with SST differences defined between the eastern Mediterranean and Indian basins (the northern and southern tropical Atlantic) with (left) and without(right) linear trends. Values below |0.25| are not displayed.

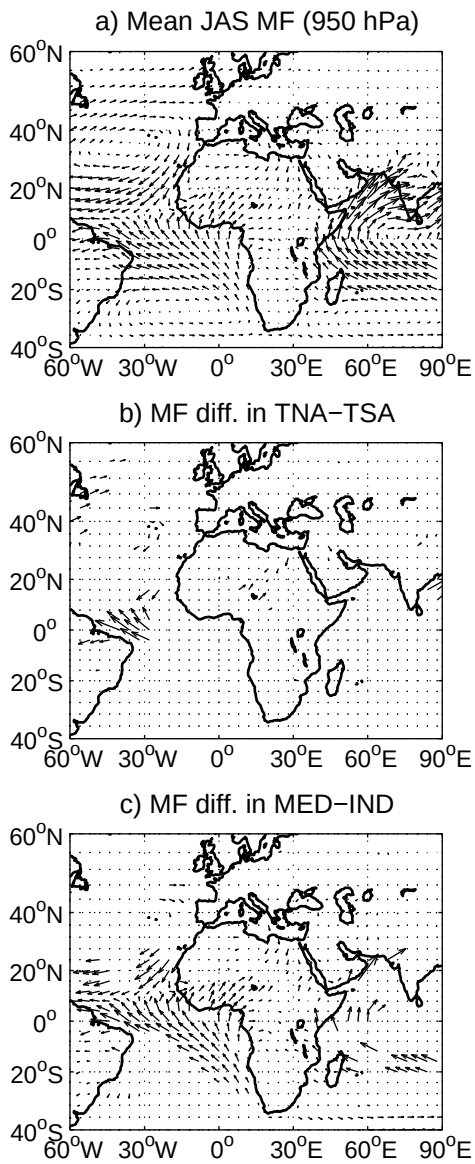

Figure 7. July-September moisture flux at 950 hPa over the period 1920-2008. (a) mean values; (b) significant differences between the northern and southern tropical Atlantic basins; (c) significant differences between the eastern Mediterranean basin and the Indian Ocean. The statistical significance has been estimated on the zonal and meridional components through a Student t-test contrasting the 20 highest and the 20 lowest seasonal differences versus all the remainders.

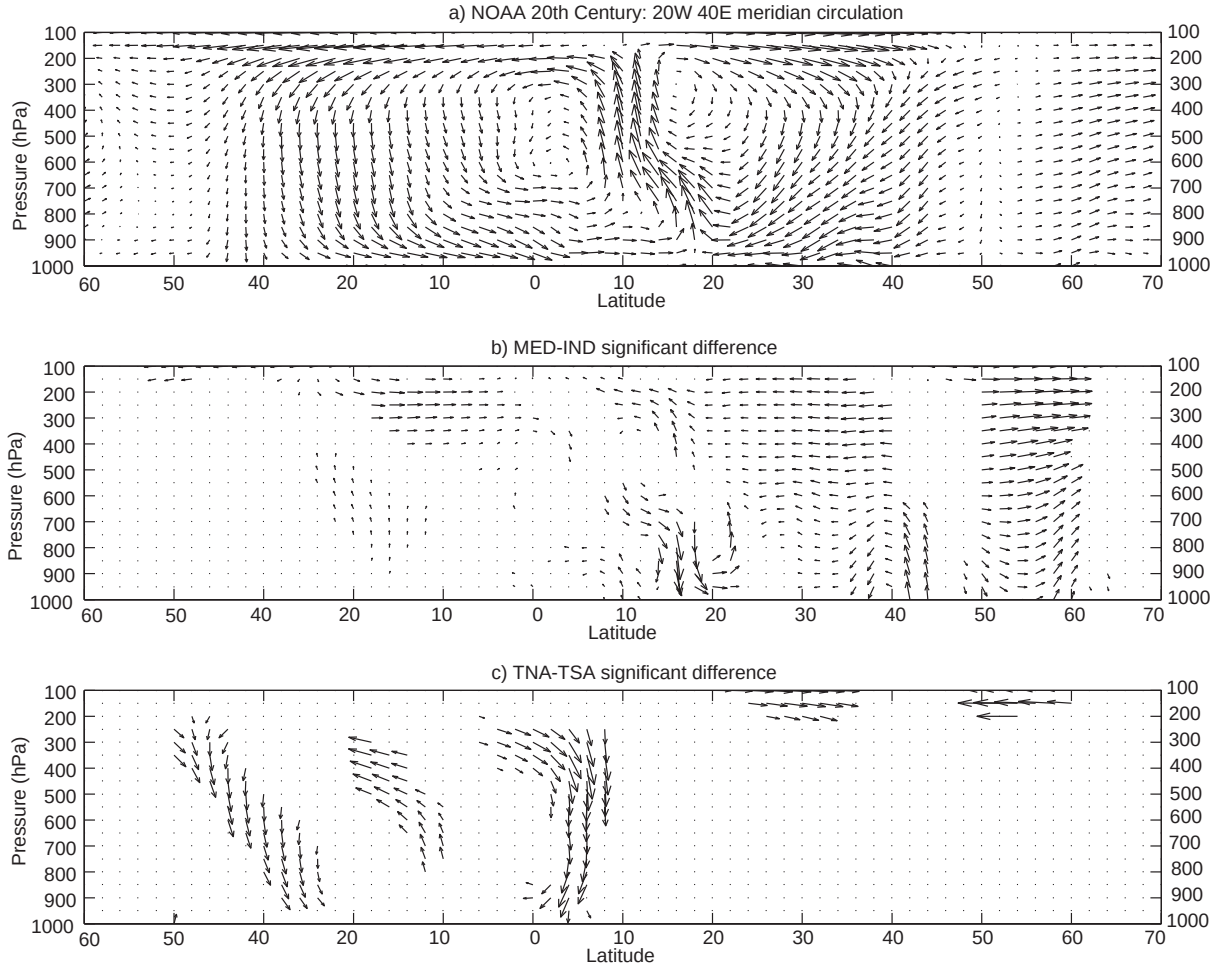

Figure 8. July-September atmospheric circulation (divergent wind, -ω) along a meridional-vertical plane averaged between 20°W and 40°E over the period 1920-2008. (a) Mean values; (b) MED-IND composite relative to SST differences between the eastern Mediterranean basin and the Indian Ocean (c) TNA-TSA composite relative to SST differences between the northern and southern tropical Atlantic basins. In panels (b,c) only the significant values are displayed. The statistical significance has been estimated on the vertical and meridional components through a Student t-test contrasting the 20 highest and the 20 lowest seasonal differences versus all the remainders.

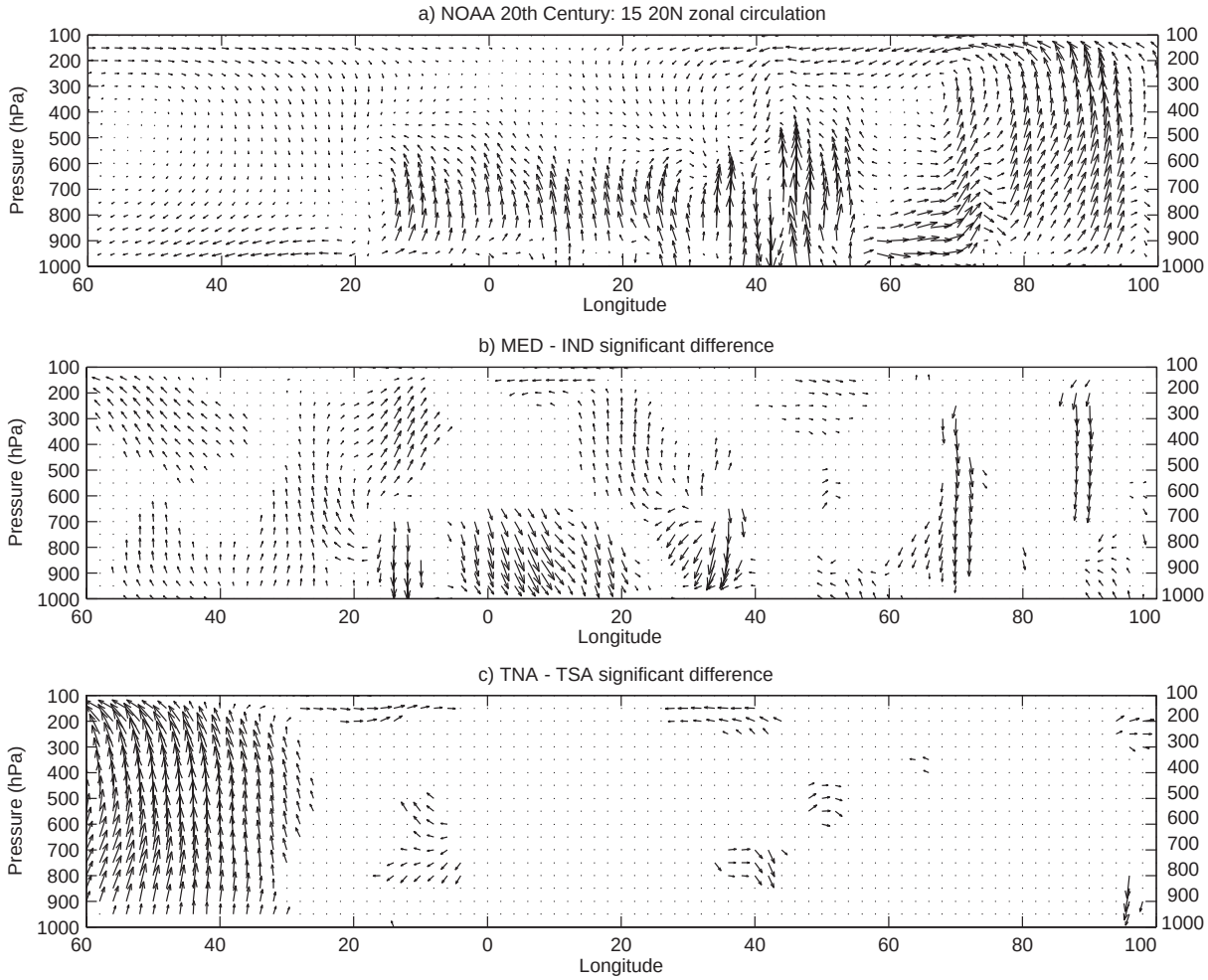

Figure 9. As figure 8 but for the July-September atmospheric circulation along a zonal-vertical plane averaged between 15°N and 20°N.